Crystal Engineered Albendazole with Improved Dissolution and Material Attributes

Amitha Thakur, Rajesh Thipparaboina, Dinesh Kumar, Kodukula Sai Gouthami, Nalini R Shastri*

Solid State Pharmaceutical Research Group (SSPRG), National Institute of Pharmaceutical Education and Research, Hyderabad, India

*Corresponding author. Nalini Shastri

Tel. +91-040-23423749

Fax. +91-040-23073751

E-mail: nalini.niperhyd@gov.in , svcphod@yahoo.co.in

Address: Department of Pharmaceutics, NIPER (National Institute of Pharmaceutical Education & Research), Balanagar, Hyderabad, India, Pin Code – 500037

Electronic supplementary information (ESI)

Glossary

1.0 Methods for crystal morphology prediction in vacuum

Based on the solubility studies, simulation study was carried out using software tool, MATERIAL STUDIO 6.1., Accelrys Inc., San Diego, CA. Selection of appropriate forcefield and description of charge set is very essential in modeling of morphology. Three models were used to predict crystal morphology in vacuum. First BFDH model was used to list possible growth faces as it is predominantly used regardless of its low accuracy[1]. Second, growth morphology model was used to calculate attachment energy of each facet obtained from BFDH model[2]. Third, equilibrium morphology model was used to determine surface energies for all relevant crystal faces at 0 K.

2.0 Crystal habit prediction with effect of solvent

Layer docking approach examines the effect of additives on the individual crystal faces, which are cleaved from a pure crystal. If the additive has inadequate interaction on special face, then the growth rate of that face will be higher and this face will become smaller when compared to other faces or this face may disappear[3]. Material studio software package was used to run the calculations (Materials Studio 6.1., Accelrys Inc., San Diego, CA) for layer docking. From the crystallographic information file, initially the unit cell was constructed and then optimized. Smart minimiser was used to perform minimization on the unit cell using Discover tool. Crystal habit in vacuum predicted by AE model gave information containing multiplicities, interplanar distances, facet areas and attachment energy. These morphologically important lattice parameters were used for amorphous cell construction and cleaved parallel to the (h k l) plane at depth of four unit cell. Crystal structure layer was constructed as periodic superstructure of 3 × 2 unit cells. Next, the crystal structure layer was optimized by molecular mechanics and dynamics. Acetone and ethyl acetate with dielectric constant of 33, 20.7 and density of 0.791, 0.897 g/mL respectively were chosen for the simulation study.

Subsequently, amorphous construct tool was used to construct solvent layer containing 45 ethyl acetate molecules by using lattice parameters of the faces obtained from attachment energy model. Amorphous cell was minimized by smart minimiser using Newton method with 10,000 iterations at medium quality. In the next step, NVE (N= constant number of particles, V= constant volume, E = constant energy), NPT (P = constant pressure, T= constant temperature) were performed for equilibration. This solvent layer was adsorbed onto the crystal surface layer with vacuum slab of 10 A^0 above the solvent layer to eliminate the effect of free boundaries. Constraints were fixed for crystal structure layer and were not allowed to relax during

simulation, while solvent molecules were allowed to move. Molecular dynamic simulation was performed using Nose algorithm and Andersen[4] as temperature control method which chooses atom collision times from a Poisson distribution at each time step and changes their velocities according to the Boltzmann distribution. Energy minimization was carried out for the interfacial layer. In the next step, molecular dynamic simulation was carried out using NVT ensemble for 10 ps at a time step of 1 fs. Again, the layer was minimized wherein the obtained potential energy was sum of crystal structure layer and solvent layer designated E_{total}. Energy of the crystal structure layer and solvent layer was denoted as $E_{surface}$ and $E_{amorphous}$, respectively. Similarly, simulation was also performed using 100 acetone molecules separately.

For the equilibration stage, the time step for the MD simulation was 1 fs with a period of 60 ps. The Columbic and Vander Waals interactions were calculated by employing the standard Ewald summation[5]. After equilibration stage, production stage was performed. Modified attachment energy was then calculated by the formula which was used to correct the vacuum attachment energy

$$^{Mod}E_{att} = E_{total} - (E_{surface} + E_{amorphous})$$

From the modified attachment energy, aspect ratio and % total facet area of each face was calculated.

Readers can refer to our previous papers regarding crystal habit simulation methodology and basic pharmaceutical aspects[6-10].

2.0 Solid state characterization

2.1 Microscopy

Inverted microscope (Nikone TiU) operating with NIE software was used to observe the crystals at different magnifications. Aspect ratio (defined as the ratio of length to width) and particle sizes were also determined (n = 10). Surface morphology of optimized batches was observed by taking photographs of samples in Hitachi S-300 N SEM at a voltage of 15 kV. Beforehand, the samples were mounted on alumina stubs using double adhesive tape. Photomicrographs were taken for each sample at different magnifications.

2.2 Differential scanning calorimetry

Mettler Toledo DSC system operating with STARe software was used for thermal analysis. Samples weighing 5-10 mg were heated in sealed aluminium pans with pin hole were scanned at 10 °C/min over a temperature range of 25–250 °C in nitrogen environment purged at a flow rate of 80 mL/min.

2.3 FTIR

Accurately weighed 2 mg of samples were mixed thoroughly with 100 mg of potassium bromide IR powder (1-2% w/w sample/alkali halide) and compressed under vacuum at a pressure of 12 psi for 3 min. The resultant pellet was affixed in a suitable holder and the FTIR spectra were recorded in the range 4000 to 400 cm^{-1}.

2.4 P-XRD

P-XRD of samples was carried out using Ni filtered Cu-Kα radiation (wavelength = 1.5406 Å). The data were recorded over an angular range of 2° to 50°, 2θ at step time of 0.030 steps/0.5 s. All P-XRD measurements were done at ambient temperature.

Supplementary Tables

Table 1SI. Qualitative solubility of ABZ in different solvents

Solvent	**Solubility (mg/mL)**
DMSO	33.33 ± 5.03
DMF	12.50 ± 8.22
Methanol	16.66 ± 1.132
Acetone	8.03 ± 3.40
EA	10.00 ± 2.63
Chloroform	12.50 ± 4.25
DCM	3.33 ± 2.887
Petroleum ether	8 ± 2.00
n-hexane	10± 2.00

Table 2SI. Study of process parameters on Albendazole spherical agglomerates

S. No	**Amount of solvent in mL**			**Stirring parameters**		**Temperature (^{0}C)**
	DCM	Acidified methanol	Water	Speed (rpm)	Time (min)	
1	3.4	22.5	24.1	400	20	RT
2				500	30	25
3				600	40	30
4				700	50	35
5				800	60	40
6				900	80	45

Table 3SI. % TFA (total facet area) of ABZ crystals from different simulation studies

Faces	**% Total facet area**				
	BFDH	AE	EM	ethyl acetate	acetone
(2 0 0)	40.337	40.403	15.487	15.709	9.312
(0 0 2)	30.519	34.856	14.690	29.839	-
(2 0 -2)	6.923	9.0529	19.029	-	18.846
(1 1 0)	10.929	5.703	-	-	-
(1 1 -1)	7.500	7.680	-	9.790	-
(1 1 1)	3.792	2.305	-	44.661	71.842
(2 0 2)	-	-	18.020	-	-
(3 1 -3)	-	-	5.256	-	-
(3 1 3)	-	-	3.818	-	-

Key: BFDH**-** Bravais, Friedel, Donnay and Harker model, AE- Attachment energy model, EM- equilibrium morphology model

Table 4SI. Effect of process parameters, polymers and amount of bridging liquid on ABZ spherical agglomerates.

Speed (rpm)	Sph	Stirring time (min)	Sph	Temp (°C)	Sph	Additive type	% w/v	Sph	BL (mL)	Observation	Sph
400	0.91 ±0.15	20	-	RT	Coarse particles	HPC	0.5	1.06±0.11	1.0	Fines	-
500	0.92± 0.19	30	-	25	1.03 ±0.31		1	0.94±0.10	2.0/3.0	Powdery	-
600	0.89± 0.19	40	1.06 ±	30	0.94 ±0.22	HPMC	0.5	0.92±0.42	3.4	Spherical agglomerates	1.02±0.17
700	0.83± 0.21	60	1.17 ±0.30	35	0.78 ±0.25		1	0.90±0.39	4.0	Irregular agglomerates	0.57±0.11
800	-	80	0.95 ±0.14	40	0.84 ±0.17	PVP	0.5	Coarse particles	4.75	pasty mass at the bottom	-
900	-	-	-	45	Fines		1		4.95	Pasty mass	-

Key: Sph-Sphericity, BL-Bridging liquid

Table 5SI. Density and flowability of ABZ and modified crystals

Product code	Bulk density (g/cm^3)	Tapped density (g/cm^3)	Angle of repose (θ)	Hausners ratio	Carr's index
ABZ	0.376	0.573	37.04	1.52	34.3
ABZ-EA	0.228	0.280	22.75	1.22	18.5
ABZ-AC	0.264	0.354	24.04	1.34	25.4
ABZ-SA	0.246	0.352	21.04	1.42	29.9
ABZ-SA-HPC	0.269	0.312	16.21	1.15	13.5

Supplementary Figures

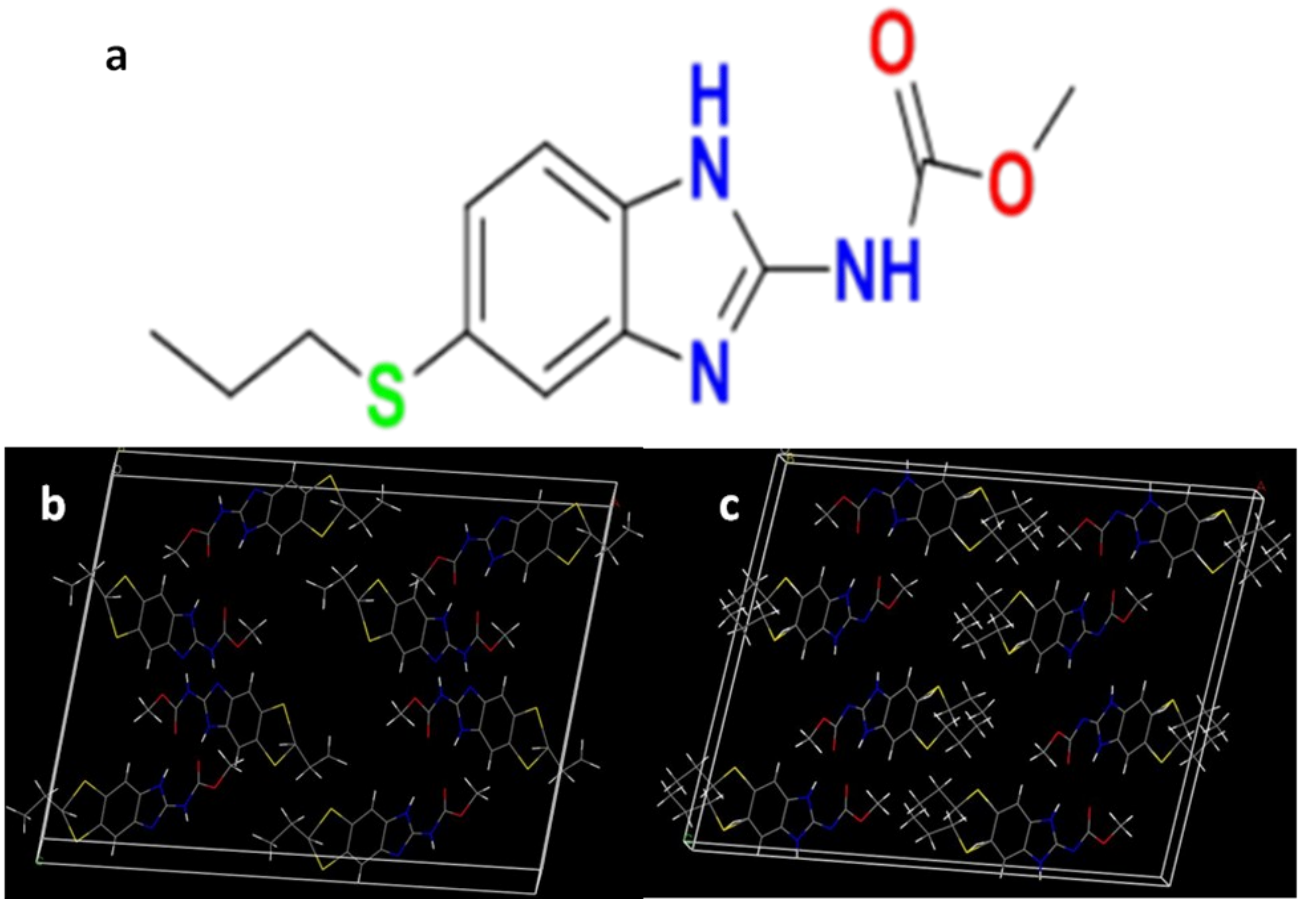

Figure 1SI a) Chemical Structure b) Crystal structure of ABZ Form I and c) Crystal structure of ABZ Form II

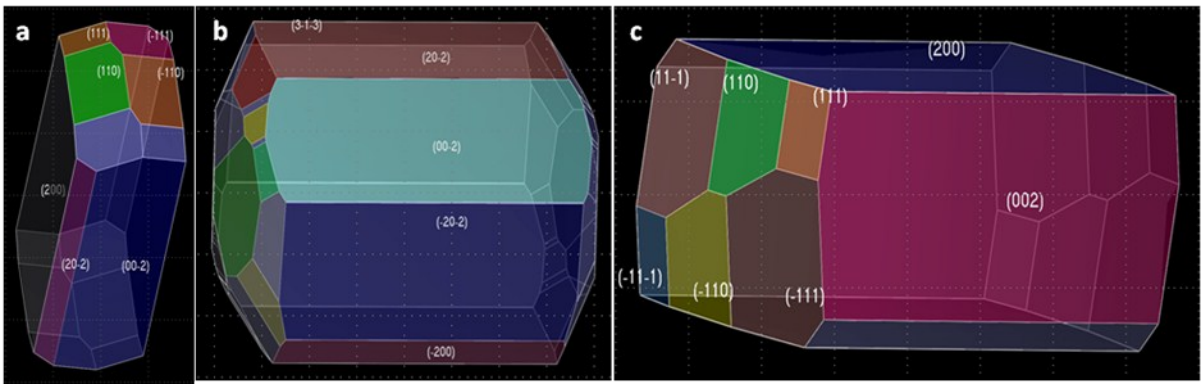

Figure 2SI Predicted vacuum morphology of ABZ by a) BFDH model b) Equilibrium morphology model c) Growth morphology model

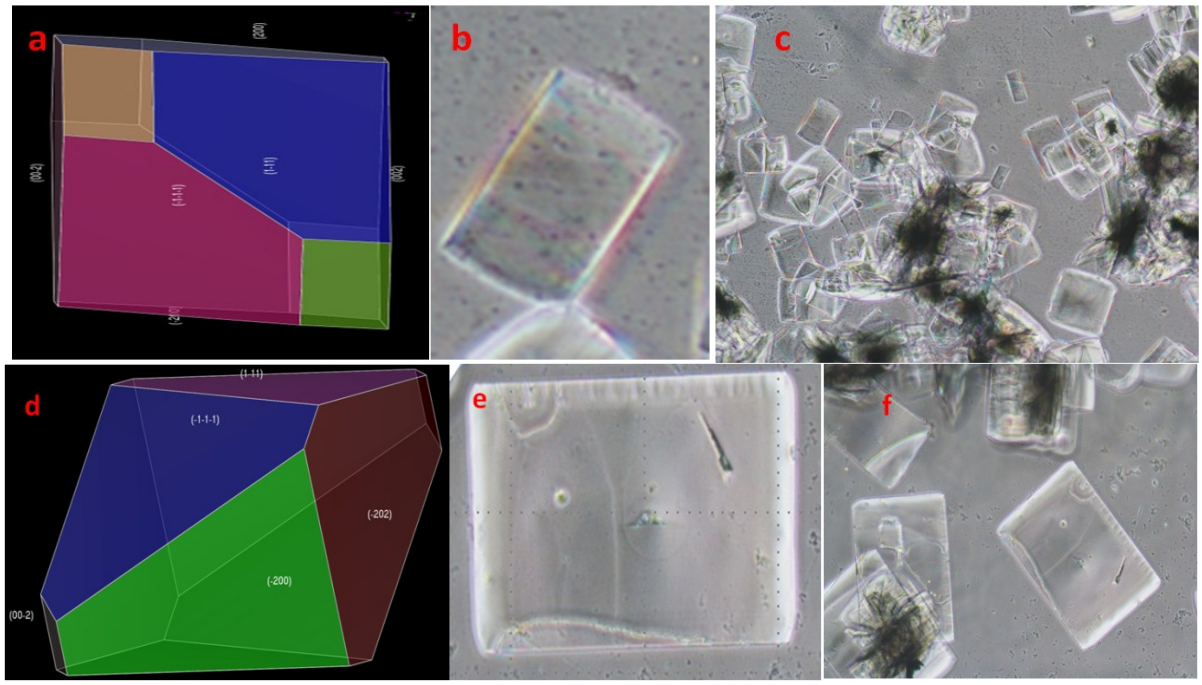

Figure 3SI Simulated (a) & experimental crystal habit of ABZ-EA (b,c), Simulated (d) & experimental ABZ-AC (e,f).

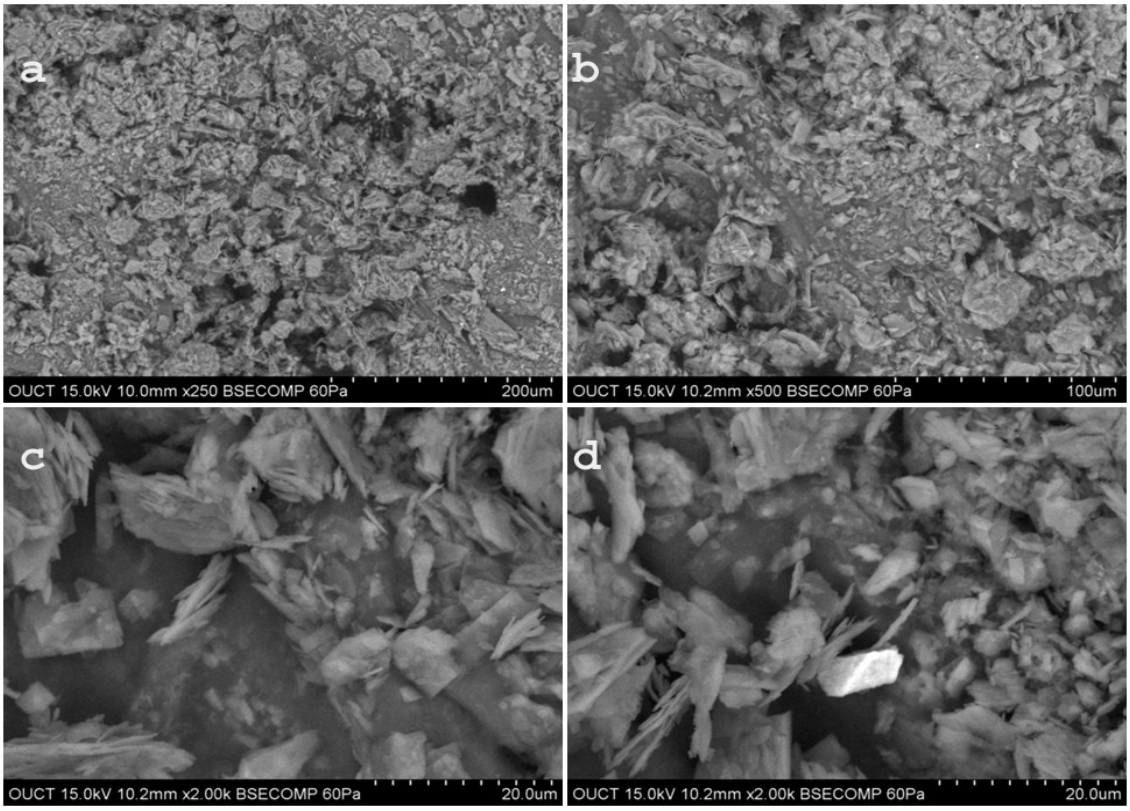

Figure 4SI SEM images of ABZ at a) 250x, b) 500 x, c) 2000 and d) 2000 x magnification

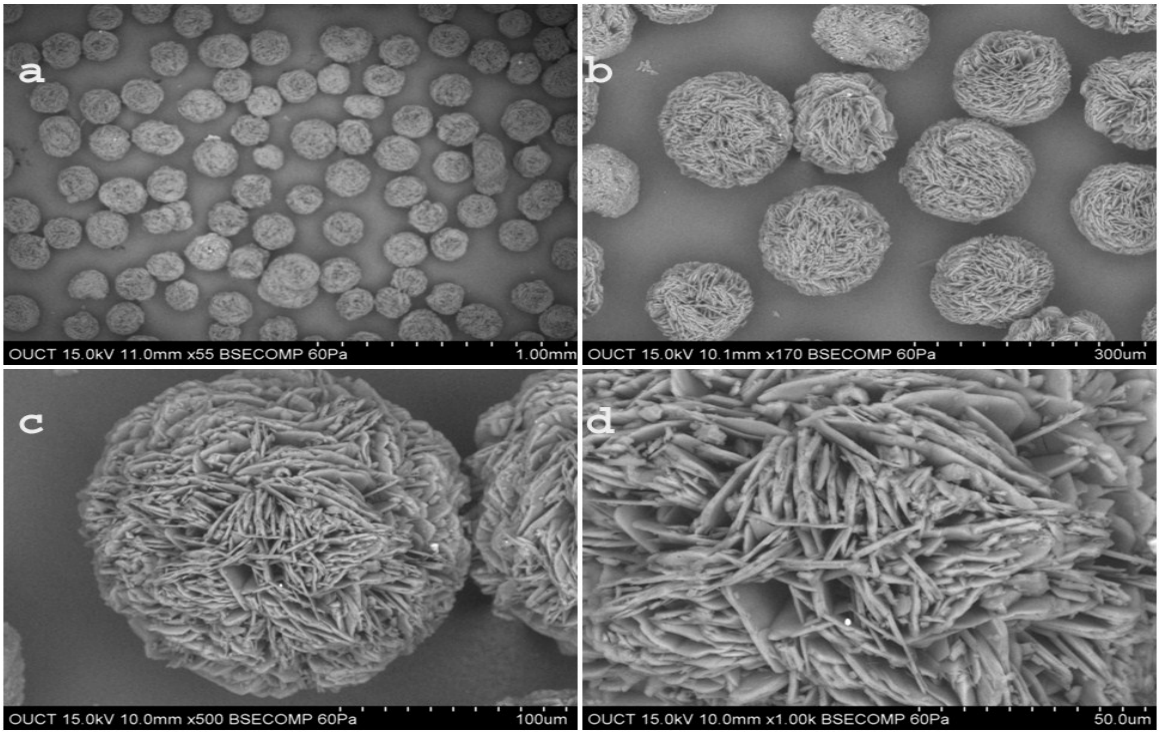

Figure 5SI SEM images of ABZNB at 55 x (a), 170 x (b), 500 x (c), 1000 x (d) magnification

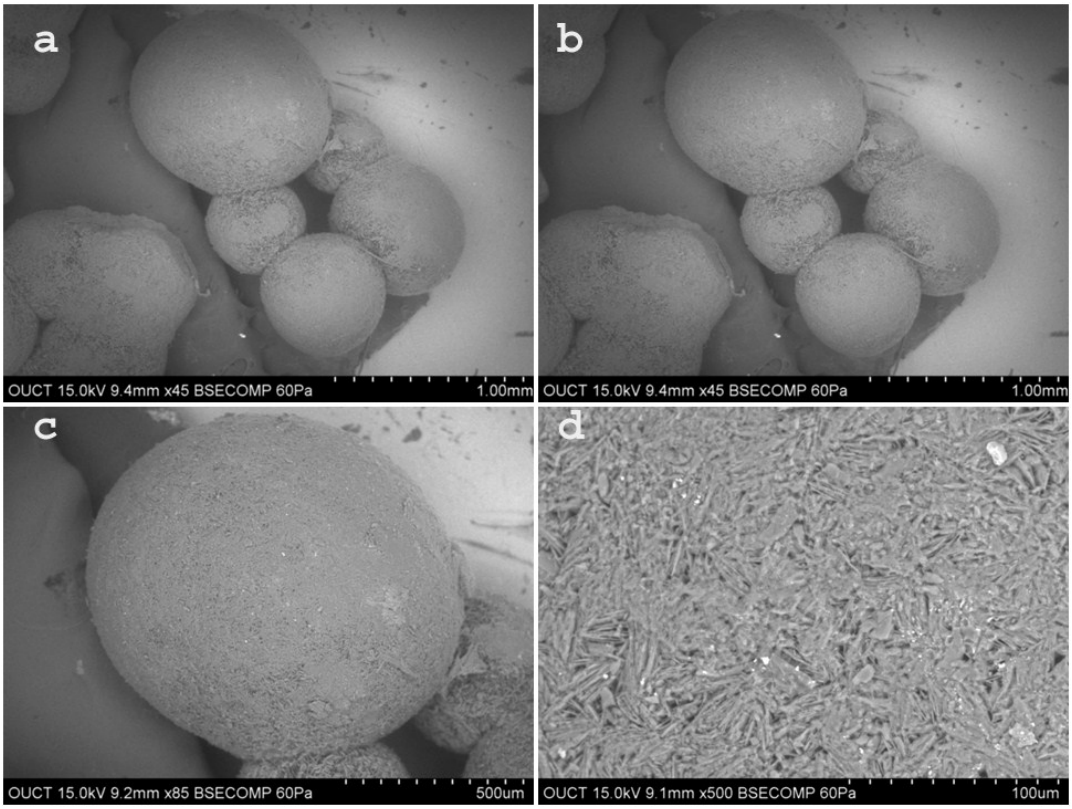

Figure 6SI SEM images of 45 x (a,b), 85 x (c), 500 x (d) magnification respectively

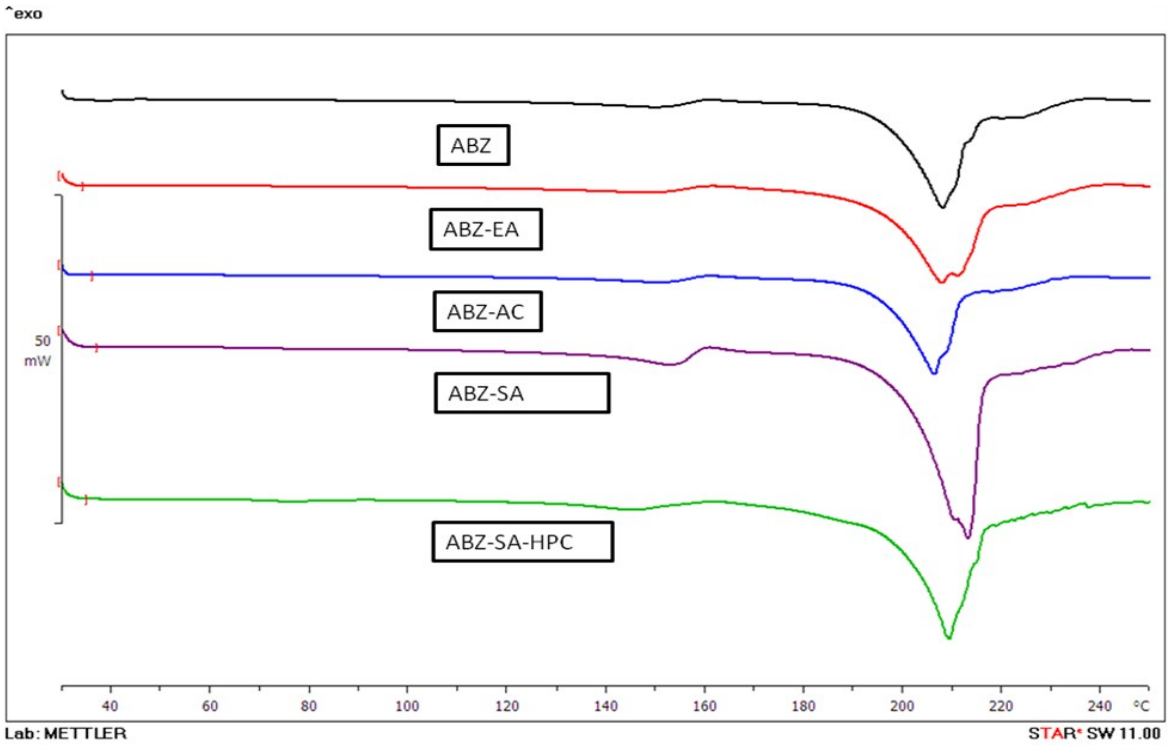

Figure 7SI Overlay of DSC thermograms of ABZ and modified crystals

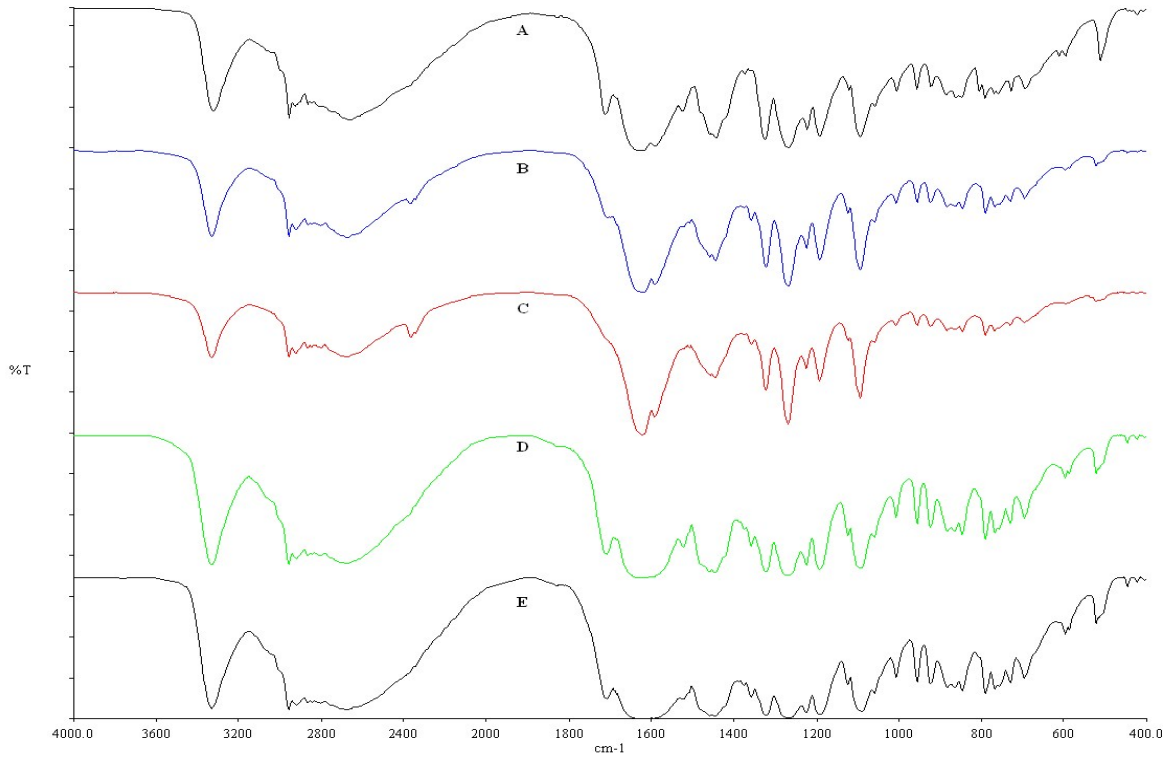

Figure 8SI FTIR spectra of a) ABZ b) ABZ-EA c) ABZ-AC d) ABZ-SA e) ABZ-SA-HPC

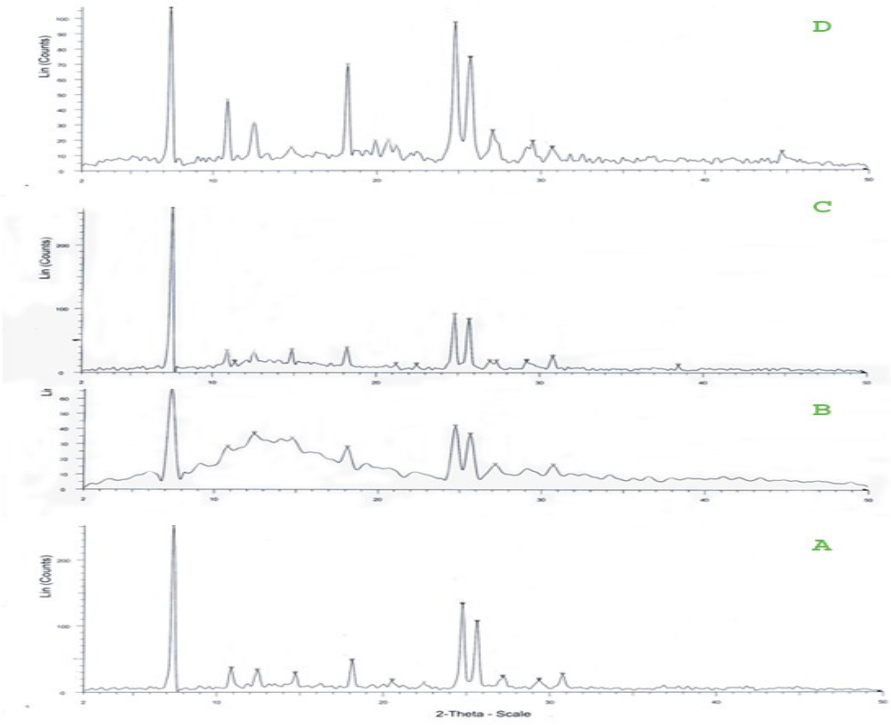

Figure 9SI Overlay of p-XRD diffractograms a) ABZ b) ABZ-EA c) ABZ-AC d) ABZ-SA-HPC

References

1. A. Bravais, *Etudes cristallographiques*, Gauthier-Villars, 1866.
2. P. Hartman and P. Bennema, *J.Cryst. Growth*, 1980, **49**, 145-156.
3. Z. Berkovitch-Yellin, J. Van Mil, L. Addadi, M. Idelson, M. Lahav and L. Leiserowitz, *J.Am. Chem. Soc.*, 1985, **107**, 3111-3122.
4. H. C. Andersen, *J. Chem. Phys.*, 1980, **72**, 2384.
5. P. Ewald, *Ann. Phys*, 1921, **64**, ll.
6. A. Thakur, D. Kumar, R. Thipparaboina and N. R. Shastri, *J Cryst Growth*, 2014, **406**, 18-25.
7. D. Kumar, R. Thipparaboina, S. R. Modi, A. K. Bansal and N. R. Shastri, *CrystEngComm*, 2015, **17**, 1615-1624.
8. D. Kumar, R. Thipparaboina, B. Sreedhar and N. R. Shastri, *CrystEngComm*, 2015, **17**, 6646-6650.
9. D. Kumar, R. Thipparaboina, S. R. Modi, A. K. Bansal and N. R. Shastri, *J Cryst Growth*, 2015, **422**, 44-51.
10. K. S. Gouthami, D. Kumar, R. Thipparaboina, R. B. Chavan and N. R. Shastri, *Int J Pharm*, 2015, **491**, 26-34.